

# GANs for LIFE: Generative Adversarial Networks for Likelihood Free Inference

Vinay Jethava

Devdatt Dubhashi

Computer Science and Engineering Department,  
Chalmers University of Technology, Sweden

## Abstract

We introduce a framework using Generative Adversarial Networks (GANs) for likelihood-free inference (LFI) and Approximate Bayesian Computation (ABC). Our approach addresses both the key problems in likelihood-free inference, namely how to compare distributions and how to efficiently explore the parameter space. Our framework allows one to use the simulator model as a black box and leverage the power of deep networks to generate a rich set of features in a data driven fashion (as opposed to previous ad hoc approaches). Thereby it is a step towards a powerful alternative approach to LFI and ABC. On benchmark data sets, our approach improves on others with respect to scalability, ability to handle high dimensional data and complex probability distributions.

## 1 Introduction

Generative Adversarial Networks (GANs), introduced by Goodfellow et al. [2014], have become recognized as a powerful framework for generative models for complex target distributions with an impressively wide range of applications in diverse domains such as vision, natural language and causal reasoning [see Goodfellow, 2016, and references therein]. Recently, several variations of the GAN model having alternative distance functions and architectures have been introduced [Dziugaite et al., 2015, Arjovsky et al., 2017].

In this paper, we adapt the GAN framework for likelihood-free inference (LFI) and Approximate Bayesian Computation (ABC). The likelihood func-

tion  $\mathcal{L}(\theta) = P(\mathbf{X} \mid \theta)$  plays a central role in statistics and machine learning. However, in many applications, the model may be too complex to evaluate analytically or computationally intractable to even approximate numerically. Complex simulators are used in many areas of science as models of the underlying phenomena of interest. In such cases, the likelihood function may only be available implicitly via samples generated by the complex simulation model for an appropriate setting of parameters. Standard inference methods are not applicable in such cases, but inference may still be possible via data simulated from the model [see Lintusaari et al., 2017, for a recent review]. There have been two major approaches to LFI and ABC, one based on MCMC methods and the other based on Bayesian Optimization, see section 2.1 for a short overview.

We introduce a third powerful approach to LFI and ABC employing the GAN framework<sup>1</sup>. We show that the GAN approach provides a computationally efficient way to address the two major challenges in LFI, namely, (1) to compare two empirical distributions and (2) to explore the parameter space effectively. We use *Maximum Mean Discrepancy* (MMD), a well grounded *integral probability metric* based on kernel embeddings in Reproducing Kernel Hilbert Space (RKHS) as a unifying concept to address both problems. First, it is a statistically sound approach to compare two probability distributions. Second, it is differentiable and hence can be used in the GAN framework to generate gradients to train the generator [Dziugaite et al., 2015]. Our approach uses a proxy network to approximate an arbitrarily complex simulator in a black box fashion to create an end-to-end differentiable system for LFI.

Our method has several advantages over other approaches as we demonstrate in our experimental re-

<sup>1</sup>In an updated version of their earlier manuscript [Gutmann et al., 2017, page 12], the authors make the following retrospective comment: “the method of Goodfellow et al. [2014] is a method for producing random samples while ours is a method for statistical inference.”

---

**Algorithm 1** ABC algorithm
 

---

```

for  $i = 1$  to  $N$  do
    repeat
        Propose  $\theta \sim P_\theta(\theta)$            {Affects speed}
        Generate  $\mathbf{Y}_\theta \sim P(\mathbf{Y}_\theta|\theta)$  {Simulator}
    until  $\mathbf{X} \simeq \mathbf{Y}_\theta$            {Affects quality}
    Set  $\theta_i = \theta$ 
end for
    
```

---

sults:

- We gain computational efficiency in running time (Section 3.1.1) in parameter inference as well as in generating posterior samples.
- We show that our method is able to deal with low probability regions of the parameter space (Section 3.1.2).
- Our method gracefully scales to higher dimensional parameter spaces (Section 3.1.3).
- We can use the simulator as is, in a black box fashion without the need to recode it as in Moreno et al. [2016].
- We can use the power of deep networks to learn complex feature representations to create summary statistics in a data driven fashion rather than *ad hoc* approaches tied to specific parametrized families (Sections 3.2 and 3.3).
- Finally, we can leverage the recent advances in the field of deep learning, and the wide availability of powerful frameworks such as TensorFlow and PyTorch to make the GAN approach readily accessible to a wider community of researchers using LFI and ABC.

## 2 Background and Related Work

### 2.1 Likelihood-Free Inference and ABC

Formally, likelihood-free inference learns the parameter  $\theta$  by generating simulated data  $\mathbf{Y}_\theta$  and accepting proposals (for the parameter  $\theta$ ) when the simulated data resembles the true data  $\mathbf{X}$ . Algorithm 1 shows the basic ABC algorithm.

There are several challenges when doing LFI-based parameter inference: (1) the choice of distance measure  $d(\cdot, \cdot)$  between the observed data ( $\mathbf{X}$ ) and the simulated data ( $\mathbf{Y}_\theta$ ) is crucial to the quality of the inference; (2) the acceptance threshold for selecting parameter  $\theta$  which generates simulated data resembling the observed data (i.e.,  $d(\mathbf{Y}_\theta, \mathbf{X}) \leq \epsilon$ ) is very low, hence

the search in parameter space has to be very efficient; and, (3) generating the simulated data  $\mathbf{Y}_\theta$  may be a computationally intensive process.

Several attempts have been made to address this problem. Often, a low-dimensional summary statistic  $T$  is chosen to represent the data so that the distance  $d(\mathbf{X}, \mathbf{Y}_\theta)$  can be computed in terms of the summary statistic  $d_T(t_{\mathbf{X}}, t_{\mathbf{Y}})$  [see, e.g., Pritchard et al., 1999]. The choice of the summary statistic is crucial and hitherto has been largely intuition-driven without formal justification. For exploring the parameter space, two major approaches are advanced Monte Carlo methods [Marjoram et al., 2003, Beaumont et al., 2009, Moreno et al., 2016] to explore parameters  $\theta$  resulting in better acceptance ratios, and more recently, approaches based on Bayesian optimization (BOLFI) [Gutmann et al., 2016].

In a series of recent papers [Gutmann et al., 2014, 2017, 2016], the authors have suggested two novel ideas: (1) Treating the problem of discriminating distributions as a classification problem between  $\mathbf{X}$  and  $\mathbf{Y}_\theta$ ; and (2) regression of the parameter  $\theta$  on the distance-measure  $d_T(\cdot, \cdot)$  using Gaussian Processes in order to identify the suitable regions of the parameter space having higher acceptance ratios.

### 2.2 Maximum Mean Discrepancy

The Maximum Mean Discrepancy (MMD) is an integral probability metric defined via a kernel  $k$  and its associated Reproducing Kernel Hilbert Space (RKHS) [Muandet et al., 2017, Sriperumbudur et al., 2012, Gretton et al., 2007]. Explicitly, the MMD distance with kernel  $k$  between distributions  $P$  and  $Q$  is given by

$$\begin{aligned} \text{MMD}(k, P, Q) := & E[k(X, \tilde{X})] - 2E[k(X, Y)] \\ & + E[k(Y, \tilde{Y})] \end{aligned}$$

where  $X, \tilde{X}$  are independent copies from  $P$  and  $Y, \tilde{Y}$  are independent copies from  $Q$ . For empirical samples  $X := \{x_1, \dots, x_m\}$  from  $P$  and  $Y := \{y_1, \dots, y_n\}$  from  $Q$ , an unbiased estimate of the MMD is  $\widehat{\text{MMD}}(k, X, Y) := \frac{1}{m(m-1)} \sum_{i,i'} k(x_i, x_{i'}) - \frac{2}{mn} \sum_{i,j} k(x_i, y_j) + \frac{1}{n(n-1)} \sum_{j,j'} k(y_j, y_{j'})$ .

As shown in Dziugaite et al. [2015], this can be differentiated with respect to parameters generating one of the distributions.

section LFI using the GAN Model Consider a target distribution  $P(\mathbf{X}|\theta)$  with unknown parameters  $\theta_0 \in \mathbb{R}^d$  that need to be estimated. We have access to a black box simulator  $S : (\theta, \epsilon) \rightarrow \mathbf{X}$  allowing us to generate samples from the distribution for any choice

**Algorithm 2** ABC-GAN:  $\alpha = 10^{-3}$ ,  $m = 50$ 


---

```

1: while  $\theta^g$  is not converged do
2:   for  $i = 0$  to  $m$  do
3:     Draw sample  $\theta^{(i)} \sim P_\theta(\theta)$ 
4:     Draw noise sample  $\epsilon^{(i)} \sim \epsilon$ 
5:     Sample from real data  $\mathbf{x}^{(i),r} \sim \mathcal{O}$ 
6:     Generate new parameter  $\theta^{(i),g} \leftarrow G_u(\theta^{(i)})$ 
7:     Simulator sample  $\mathbf{x}^{(i),s} \leftarrow \mathcal{S}(\theta^{(i)}, \epsilon^{(i)})$ 
8:     Approximator sample  $\mathbf{x}^{(i),a} \leftarrow A_v(\theta^{(i)}, \epsilon^{(i)})$ 
9:   end for
10:   $\mathcal{L}_v^A \leftarrow MMD(\{\mathbf{x}^{(i),a}\}, \{\mathbf{x}^{(i),s}\})$ 
11:   $\mathcal{L}_w^D = \frac{1}{m} \sum_i (\log D(\mathbf{x}^{(i),r}) + \log D_w(1 - \mathbf{x}^{(i),a}))$ 

12:   $\mathcal{L}_u^G = \frac{1}{m} \sum_{i=1}^m \log(1 - D_w(A_v(G_u(\theta^{(i)}))))$ 
13:  Update  $v \leftarrow v + \alpha \cdot \text{RMSPProp}(\nabla_v \mathcal{L}_v^A)$ 
14:  Update  $u \leftarrow u + \alpha \cdot \text{RMSPProp}(\nabla_u \mathcal{L}_u^G)$ 
15:  Update  $w \leftarrow w + \alpha \cdot \text{RMSPProp}(\nabla_w \mathcal{L}_w^D)$ 
16: end while
    
```

---

of parameter  $\theta$ . Here, we have captured the underlying stochasticity of the simulator using suitable noise  $\epsilon$ . In the sequel, we use the notation  $G_u$ ,  $A_v$  and  $D_w$  to denote that the neural network units  $G$ ,  $A$  and  $D$  have the parameters  $u$ ,  $v$  and  $w$  associated with them respectively.

The stochastic and non-differentiable nature of simulator prohibits direct usage within the GAN framework. In order to address this, we introduce a new neural network unit called the ‘‘Approximator’’ with associated cost function such that it attempts to generate samples similar to the output of the simulator.

Figure 1 gives a high-level overview of the ABC-GAN architecture. The output of the generator  $\theta^g$  is concatenated with the noise  $\epsilon$  and fed into the approximator and the physical simulator. We connect the outputs of the approximator and the simulator unit to an maximum discrepancy cost [Dziugaite et al., 2015] and train the approximator unit (weights  $v$ ) such that this cost is minimized. This ensures that the distribution of the outputs generated by the approximator resembles the true simulator output [Muandet et al., 2017]. It is instructive to note that since we model the noise externally and feed it to the simulator, the simulator can be treated as a deterministic function.

The output of the approximator is fed to the discriminator and is compared against the distribution of the data in standard GAN fashion. The generator and the discriminator weights ( $u$  and  $w$  respectively) are trained separately, keeping the approximator weights constant ( $v$ ). Algorithm 2 gives the complete pseudocode for the ABC-GAN algorithm.

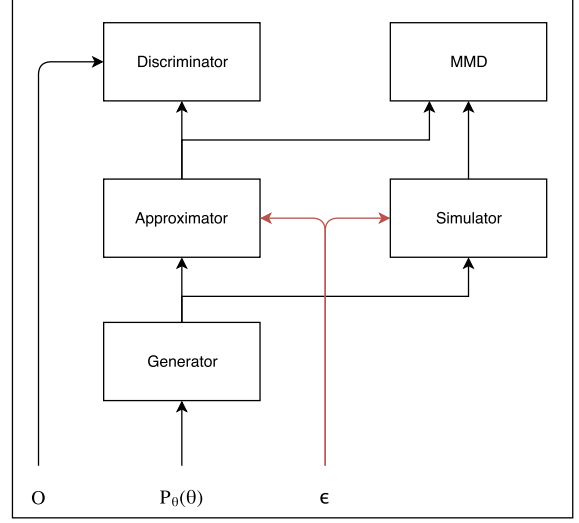


Figure 1: ABC-GAN architecture for ABC computation. The approximator output attempts to follow the output of the physical simulator in distribution due to the MMD-loss function [Dziugaite et al., 2015]. The output of the generator serves as the surrogate for the posterior distribution of the inferred parameter  $\theta$ .

We note that the choice of the discriminator is largely left to the user and it is possible to choose alternative losses for the discriminator, e.g., Wasserstein GAN [Arjovsky et al., 2017], MMD [Dziugaite et al., 2015], etc. In our experiments, we observed that training with MMDnets in lieu of the discriminator unit [Dziugaite et al., 2015] yielded the best results.

We now present two modifications to the ABC-GAN structure. Often, ABC-based methods first compute summary statistics based on the observed and the simulated samples, and use a distance metric defined on the summary statistics in order to accept or reject candidate proposals for the parameter to be inferred. In our ABC-GAN architecture, this can be easily done by introducing an additional ‘‘summarizer’’ unit between the approximator and the discriminator networks. The summarizer unit computes the summary statistics based on the output of the approximator unit and in turn, feeds them to the discriminator. However, in certain cases, the choice of the optimal summary statistic is not clear and intuition-driven guesses are the norm. The ABC-GAN architecture allows one to address this problem by data-driven learning of the summary representation. This allows easy extension to new problems where hand-engineering summary statistics might require both domain knowledge and considerable trial and error.

Method	$\hat{\mu}$	$\hat{\sigma}^2$	$t$ (in seconds)
ABC	2.92	1.17	0.147
BOLFI	2.68	1.13	2700
GAN	3.023	1.04	37.12

Table 1: We compare the results with naive ABC (using rejection sampling for 10000 samples) and BOLFI algorithm (Rejection sampling and ABC were implemented using ELFI [Kangasrääsiö et al., 2016]).

### 3 Experiments

In this section, we present several experiments to illustrate our methodology for doing ABC computation using GANs. All experiments are performed using TensorFlow r1.3 on a Macbook pro 2015 laptop with core i5, 16GB RAM and *without* GPU support. The code for the experiments will be made available on github.

#### 3.1 Synthetic Data

##### 3.1.1 Univariate normal distribution

We generate  $N = 1000$  observations from the univariate normal distribution with mean  $\mu_0 = 3$  and variance  $\sigma_0^2 = 1$ . We use the following priors:

$$\mu \sim \text{Unif}(0, 5), \quad \sigma^2 \sim \text{Unif}(1, 5), \quad (1)$$

and perform parameter estimation ( $\hat{\mu}$  and  $\hat{\sigma}^2$ ) using rejection sampling, BOLFI and ABC-GAN. Table 1 shows the timing (in seconds) and accuracy results for the three approaches. We note that BOLFI is a complex method and is unsuited for this case since generation of univariate normal samples is computationally very cheap. Nonetheless, we observe that ABC-GAN converges in reasonable time and gives comparable results to others approaches.

We also consider multi-variate normal distribution with unknown mean. Section A is the supplementary material describes the results for this model.

##### 3.1.2 Mixture of normals

We consider a mixture of two normal distributions, first studied in Sisson et al. [2007], with the observations generated from:

$$P_\theta(\theta) \sim \frac{1}{2}\mathcal{N}(0, \frac{1}{100}) + \frac{1}{2}\mathcal{N}(0, 1) \quad (2)$$

Here the second term implies large regions of low probability in comparison to the first term. Both classic rejection sampling and Monte Carlo ABC suffer from low acceptance rate and consequently, longer simulation runs (respectively, 400806 and 75895 steps) when

Method	$n_s$	$D_{KL}(p  q)$	$t$
rej. sampl. <sup>†</sup>	5000	$0.567 \pm 0.012$	0.22
ABC-GAN	5000	$0.539 \pm 0.196$	14.70
BOLFI <sup>†</sup>	1000	$0.627 \pm 0.417$	126.71
BOLFI <sup>†</sup>	5000	$0.445 \pm 0.027$	426.03

Table 2: Timing and accuracy information for the mixture of normals example averaged over 10 independent runs. The the number of samples generated by the simulator ( $n_s$ ) are shown. The Kullback-Liebler divergence ( $D_{KL}(p||q)$ ) between the true pdf ( $p$ ) and the empirical pdf estimated using accepted samples ( $q$ ) and the time taken (for the first run) in seconds ( $t$ ) are shown. <sup>†</sup>ELFI returns only negative samples so we add  $-x$  to the samples for each original sample  $x$  before computing the KL divergence.

generating samples from the low probability tail region.

In contrast, we run ABC-GAN for 5000 iterations with a mini-batch size of 10 and sequence length 10, using a learning rate  $10^{-3}$ .

Figure 2 shows the generated posterior samples and we see that the posterior samples capture the low probability component of the probability density function. We also run BOLFI [Kangasrääsiö et al., 2016] in order to compare its result to ABC-GAN.

Table 2 presents the timing and accuracy for the different methods. The accuracy is specified in terms of Kullback-Liebler divergence [Cover and Thomas, 2012] between the true pdf and the empirical pdf estimated using posterior samples in the range  $[-10, 10]$ . We note that the KL-divergence of BOLFI w.r.t. true pdf is lower compared to the KL divergence of ABC-GAN w.r.t. true pdf. However, this does not translate to capturing the low-probability space as shown in Figure 2 (b) where BOLFI does not have samples in the low-dimensional space.

We note that BOLFI fails to adequately capture the low-probability space (due to the second component) of the problem. This is reflected in Table 2. Additionally, the BOLFI implementation in ELFI is considerably slower than ABC-GAN and this scenario is exacerbated as more number of observations are provided or more simulation samples are generated due to the use of Gaussian Processes.

##### 3.1.3 Generalized linear model

Kousathanas et al. [2016] note that basic ABC algorithm and sequential Monte Carlo methods [Sisson et al., 2007, Beaumont et al., 2009] are useful for low-dimensional models, typically less than 10 parameters.

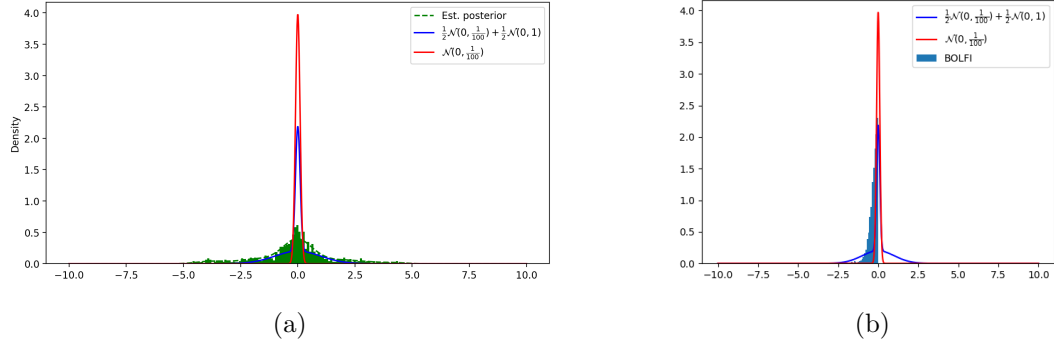


Figure 2: (a) Posterior samples for ABC-GAN (shown in green) for one run in the mixture of normals experiment (Section 3.1.2) with 5000 iterations with a mini-batch size of 10 and sequence length 10, using a learning rate  $10^{-3}$ . The probability density function for the mixture normal and the low-variability component are shown in red and blue respectively. (b) Histogram of posterior samples for first run of BOLFI. Total number of samples is 5000. We note that the low-probability space is not captured by BOLFI compared to ABC-GAN.

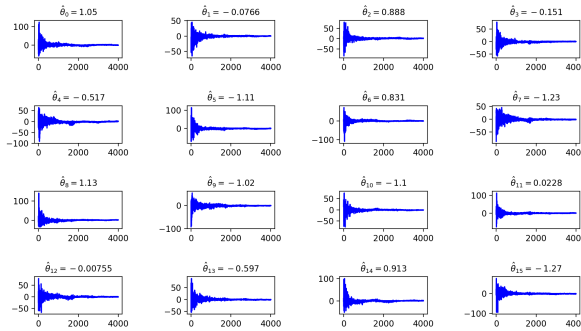


Figure 3: Inferred parameter values for one run of ABC-GAN for the GLM model (Section 3.1.3) with prior  $\theta_i \sim \text{Uniform}(-100, 100)$  and two layer feed-forward networks used for the generator and approximator in the ABC-GAN structure. The true parameter value is  $\mathbf{0}$ . We see that ABC-GAN algorithm recovers  $\hat{\theta}$  close to the true parameter  $\mathbf{0}$ .

To tackle higher dimensions, Kousathanas et al. [2016] consider scenarios where it is possible to define sufficient statistics for subsets of the parameters allowing parameter-specific ABC computation. This includes the class of exponential family of probability distributions.

In this example, we consider a generalized linear model defined by Kousathanas et al. [2016, Toy model 2] given as:

$$s = \mathbf{C}\theta + \epsilon \quad (3)$$

where  $\theta \in \mathbb{R}^n$  denotes the unknown parameter,  $\epsilon$  denote multi-variate normal random variable  $\mathcal{N}(\mathbf{0}, \mathbf{I}_n)$

and  $\mathbf{C}$  is a design matrix  $\mathbf{C} = \mathbf{B} \cdot \det(\mathbf{B}^\top \mathbf{B})^{-\frac{1}{2n}}$  and

$$\mathbf{B} = \begin{bmatrix} \frac{1}{n} & \frac{2}{n} & \cdots & \frac{1}{n} \\ 1 & \frac{1}{n} & \cdots & \frac{n-1}{n} \\ \vdots & \vdots & \ddots & \vdots \\ \frac{2}{n} & \frac{3}{n} & \cdots & \frac{1}{n} \end{bmatrix}.$$

We use a uniform prior  $\theta_i \sim \text{Uniform}(-100, 100)$  as in the original work. However, we note that Kousathanas et al. [2016] “start the MCMC chains at a normal deviate  $\mathcal{N}(\theta, 0.01\mathbf{I})$ , i.e., around the true values of  $\theta$ .” The true parameter is chosen as  $\theta = \mathbf{0}$ .

We do parameter inference for  $n = 16$  dimensional Gaussian in the above setting. Figure 12 shows the mean of the posterior samples within each mini-batch as the the algorithm progresses<sup>2</sup>. The total number of iterations is 4000 with mini-batch size of 10 and learning rate of  $10^{-2}$ . The algorithm takes 10.24 seconds. We reiterate that ABC-GAN does not use model-specific information such as the knowledge of sufficient statistics for subsets of parameters, and thus, is more widely applicable than the approach of Kousathanas et al. [2016]. Concurrently, it also enables computationally efficient inference in high-dimensional models – a challenge for Sequential Monte Carlo based methods [Sisson et al., 2007, Beaumont et al., 2009] and BOLFI [Gutmann et al., 2017].

### 3.2 Ricker’s model

The stochastic Ricker model [Ricker, 1954] is an ecological model described by the nonlinear autoregressive

<sup>2</sup>For clarity, a larger version of this plot is presented in Figure 1 of the supplementary material.



equation:

$$N^{(t)} = N^{(t-1)} r \exp\left(-N^{(t-1)} + \sigma e^{(t)}\right), \quad (4)$$

where  $N^{(t)}$  is the animal population at time  $t \in \{1, \dots, n\}$  and  $N^{(0)} = 0$ . The observation  $y^{(t)}$  is given by the distribution:

$$y^{(t)} | N^{(t)}, \phi \sim \text{Poisson}(\phi N^{(t)}), \quad (5)$$

and the model parameters are  $\theta = (\log r, \sigma, \phi)$ . The latent time series  $N^{(t)}$  makes the inference of the parameters difficult.

Wood [2010] computed a synthetic log-likelihood by defining the following summary statistics: mean, number of zeros in  $y^{(t)}$ , auto-covariance with lag 5, regression coefficients for  $(y^{(t)})^3$  against  $[(y^{(t-1)})^3, (y^{(t-1)})^6]$ . They fit a Gaussian matrix to the summary statistics of the simulated samples and then, the synthetic log-likelihood is given by the probability of observed data under this Gaussian model. Wood [2010] inferred the unknown parameters using standard Markov Chain Monte Carlo (MCMC) method based on their synthetic log-likelihood.

Gutmann et al. [2016] used the same synthetic log-likelihood but reduced the number of required samples for parameter inference based on regressing the discrepancy between simulated and observed samples (in terms of summary statistics) on the parameters using Gaussian Processes.

Our method has the following key differences compared to past approaches:

- We learn summary representation rather than using the adhoc summary statistics defined by Wood [2010].
- We use maximum mean discrepancy (MMD), a metric with well-established theoretical properties [Dziugaite et al., 2015, Muandet et al., 2017] instead of the synthetic likelihood. Other losses and other discriminator networks can be used instead of MMD.
- We explore the parameter space using stochastic gradient descent (RMSProp) instead of regression-based approach of Gutmann et al. [2016]. Other optimization algorithms (e.g., Adam) can be used alternatively.

Our method allows us to readily leverage the advances in the field of deep learning to the task of parameter inference in the ABC setting. Figure 4 shows the

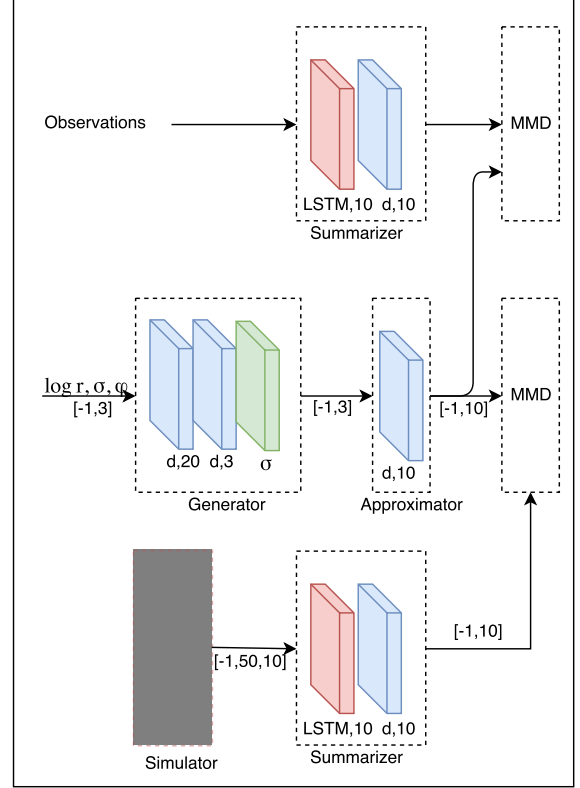


Figure 4: Network structure of ABC-GAN for the Ricker model. Here,  $[d, 10]$ ,  $\sigma$  and  $LSTM, 10$  denote a densely connected layer with 10 outputs, sigmoid activation and a LSTM with 10 units respectively.

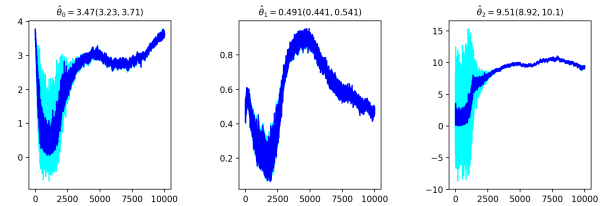


Figure 5: Inferred parameters for the Ricker model (Section 3.2) in a single run after 10000 iterations using RMSProp with learning rate= $10^{-3}$ , mini-batch size 10 and sequence length 10. The means of the estimated parameters for this run are (3.47, 0.49, 9.51) and the  $\pm 3\sigma$  range is shown.

network structure for the Ricker model. The network has the following units: <sup>3</sup>

- Generator: The generator takes as input the prior distribution on the parameters and produces as output the samples from the posterior distribution

<sup>3</sup>Please see the supplementary material for detailed description of the ABC-GAN architecture for the Ricker model.

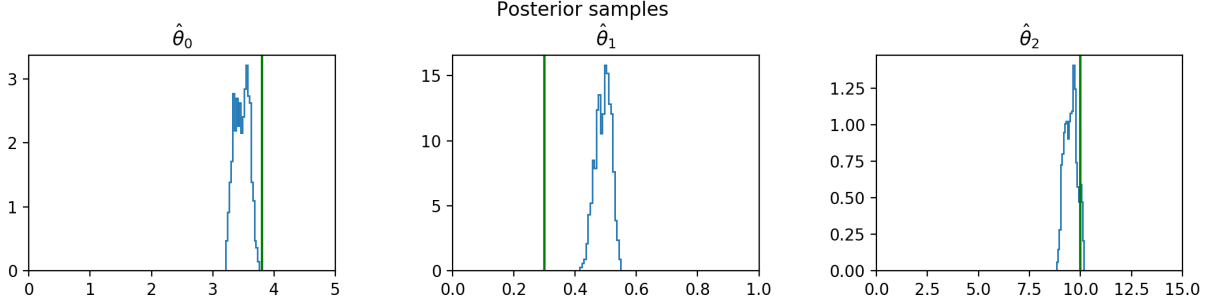


Figure 6: The histogram of the posterior samples for the last 1000 iterations of ABC-GAN in one run for the Ricker model. The true parameters (3.8, 0.3, 10) are shown in green.

on parameters under the data observed.

- **Approximator:** This unit encodes the parameters generated by the generator into the space where summary representation is projected by the summarizer.
- **Summarizer:** This unit encodes the sequences generated for given parameters values from the simulator into the summary representation.

There is another unit not shown in this schematic:

- **Decoder:** The approximator and the decoder units act as an auto-encoder. This ensures that the output of the approximator and consequently, the output of the summarizer are non-zero.

We follow the experimental setup of Wood [2010]. We simulate observations from the Ricker model with true parameters (3.8, 0.3, 10). We use the following prior distributions:

$$\begin{aligned} \log r &\sim \text{Uniform}(0, 5), \\ \sigma &\sim \text{Uniform}(0, 1), \\ \phi &\sim \text{Uniform}(0, 15). \end{aligned}$$

Figure 5 shows the output of the generator (posterior samples for the parameters) for 10000 iterations of the algorithm. A mini-batch size of 10 is used with each sequence having length 10, and the optimization is done using RMSProp with a learning rate of  $10^{-3}$ . Figure 6 shows the histogram of the posterior samples for the last 1000 iterations of the algorithm. We note that the algorithm converges and is quite close to the true parameters.

We obtain the posterior means as  $(3.185 \pm 0.249, 0.677 \pm 0.077, 11.747 \pm 0.767)$  (averaged over 10 independent runs) for the number of true observations being  $N = 50$  and an typical time of 362 seconds for 10000 iterations. BOLFI estimates the following parameters (4.12, 0.15, 8.65) for  $N = 50$  data points [see

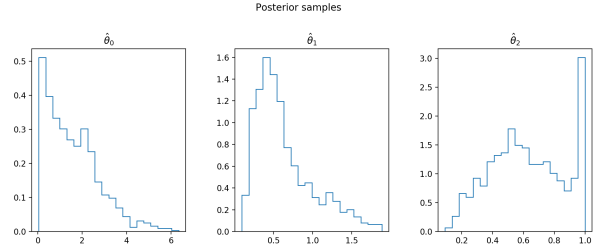


Figure 7: Result for the DCC example using the non-random features of Gutmann et al. [2017]. The true parameters are (3.6, 0.6, 0.1). A mini-batch size of 2 was used for 1000 iterations of the algorithm. The result shows the histogram of the posterior samples generated by the algorithm.

Gutmann et al., 2016, Figure 9] and a typical run of BOLFI takes 300 seconds for the given setup <sup>4</sup>.

We re-emphasize that compared to the highly-engineered features of Wood [2010], our summary representation is learnt using a standard LSTM-based neural network [Hochreiter and Schmidhuber, 1997, Graves, 2012]. Thus, our approach allows for easier extensions to other problems compared to manual feature engineering.

### 3.3 Infection in Daycare center

We study the transmission of strains of *Streptococcus pneumoniae* in a total of 611 children attending one of 29 day care centers in Oslo, Norway. The initial data was published by Vestrheim et al. [2008] and further described in a follow-up study [Vestrheim et al., 2010].

Numminen et al. [2013] first presented an ABC-based approach for inferring the parameters associated with rates of infection from an outside source ( $\Lambda$ ), infec-

<sup>4</sup>The code provided by Dr. Michael Gutmann uses the GNU R and C code of Wood for synthetic log-likelihood and is considerably faster than the python version available in ELFI.

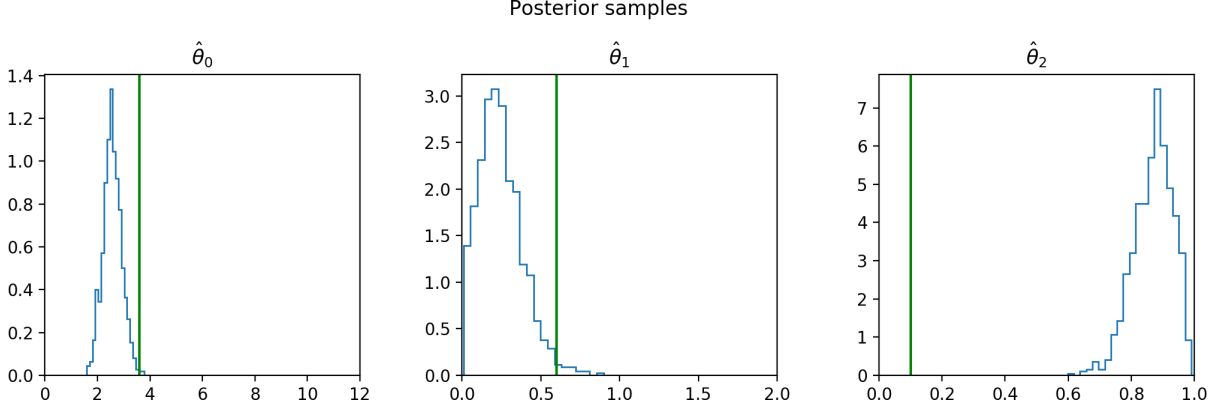


Figure 8: Histogram of the posterior samples generated by ABC-GAN for the DCC example using the convolutional summarizer. A learning rate of  $10^{-3}$  is used for 1000 iterations. The true parameters  $(3.6, 0.6, 0.1)$  are shown in green.

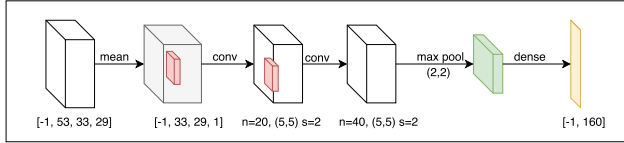


Figure 9: Convolutional summarizer for the DCC example. We generate summary representation consisting of 160 features from the input matrices  $I_{is}^{T^m}$ . The number of filters  $n$ , size of the filters  $(5, 5)$  and stride 2 are shown. The max pooling layer has size  $(2, 2)$ , and the final dense layer outputs a summary representation of size 160 for each input sample.

tion from within the DCC ( $\beta$ ) and infection by multiple strains ( $\theta$ ). Gutmann et al. [2017] presented a classification-based approach where they used classification as a surrogate for the rejection test of standard ABC method. Section C in the supplementary material presents a discussion of the hand-engineered features of Numminen et al. [2013] and Gutmann et al. [2017].

In the remainder of this section, we follow the nomenclature in [Gutmann et al., 2017]. For a single DCC, the observed data consists of presence or absence of a particular strain of the disease at time  $T^m$  when the swabs were taken. On average,  $N = 53$  individuals attend a DCC out of which only some are sampled. There are  $S = 33$  strains of the bacteria in total. So the data from each of the  $M = 29$  DCCs consists of a binary matrix with entries,  $I_{is}^t$  where  $I_{is}^t = 1$  if attendee  $i$  has strain  $s$  at time  $t$  and zero otherwise. The observed data  $\mathbf{X}$  consists of a set of  $M = 29$  binary matrices formed by  $I_{is}^{T^m}, i = 1, \dots, N_m, s = 1, \dots, 33$ . For the simulator, we use the code provided by Michael Gutmann which in turn uses the code of Elina Num-

minen<sup>5</sup>.

We assume the following prior on the parameters:

$$\begin{aligned}\Lambda &\sim \text{Uniform}(0, 12), \\ \beta &\sim \text{Uniform}(0, 2), \\ \theta &\sim \text{Uniform}(0, 1).\end{aligned}$$

We first use the non-random features defined by Gutmann et al. [2017] as our summary statistics. Figure 7 shows the histogram of the posterior samples generated by ABC-GAN using the non-random features defined by Gutmann et al. [2017]. We note that the results are not encouraging in this case, though this is an artifact of our algorithm. In order to address this, we define a new summary representation using a convolutional network. Figure 9 shows the structure of the convolutional summarizer which is used to generate summary representations instead of the non-random features defined by Gutmann et al. [2017]. The generator and approximator modules are standard one-layer feed forward networks which are fully described in Section C of the supplementary material.

Figure 8 shows the results for the convolutional summarizer. We note that the posterior samples improve especially for the parameters  $\Lambda = 3.6$  and  $\beta = 0.6$ . However, there is considerable room for improvement by using alternative summarization networks and improved training for GANs. We leave this to future work.

## 4 Conclusions

We have introduced a new approach to LFI and ABC via the GAN framework, as an alternative and comple-

<sup>5</sup><https://www.cs.helsinki.fi/u/gutmann/code/BOLFI/>



ment to the other major approaches based on MCMC and Bayesian optimization. Our GAN approach addresses both major challenges of LFI, namely comparing distributions and exploring parameter space. We argued that the ABC-GAN approach can leverage the ability of neural networks to learn summary representations in a data-driven fashion. Learning better representations, improved training of GANs and optimizing kernels for the representation are obvious directions for future work.

## References

- Martin Arjovsky, Soumith Chintala, and Léon Bottou. Wasserstein generative adversarial networks. In *International Conference on Machine Learning*, pages 214–223, 2017.
- Mark A Beaumont, Jean-Marie Cornuet, Jean-Michel Marin, and Christian P Robert. Adaptive approximate bayesian computation. *Biometrika*, 96(4):983–990, 2009.
- Thomas M Cover and Joy A Thomas. *Elements of information theory*. John Wiley & Sons, 2012.
- Gintare Karolina Dziugaite, Daniel M Roy, and Zoubin Ghahramani. Training generative neural networks via maximum mean discrepancy optimization. In *Proceedings of the Thirty-First Conference on Uncertainty in Artificial Intelligence*, pages 258–267. AUAI Press, 2015.
- Ian Goodfellow. Nips 2016 tutorial: Generative adversarial networks. *arXiv preprint arXiv:1701.00160*, 2016.
- Ian Goodfellow, Jean Pouget-Abadie, Mehdi Mirza, Bing Xu, David Warde-Farley, Sherjil Ozair, Aaron Courville, and Yoshua Bengio. Generative adversarial nets. In *Advances in neural information processing systems*, pages 2672–2680, 2014.
- Alex Graves. *Supervised sequence labelling with recurrent neural networks*, volume 385. Springer, 2012.
- Arthur Gretton, Karsten M Borgwardt, Malte Rasch, Bernhard Schölkopf, and Alex J Smola. A kernel method for the two-sample-problem. In *Advances in neural information processing systems*, pages 513–520, 2007.
- Michael U Gutmann, Ritabrata Dutta, Samuel Kaski, and Jukka Corander. Statistical inference of intractable generative models via classification. *arXiv preprint arXiv:1407.4981*, 2014.
- Michael U Gutmann, Jukka Corander, et al. Bayesian optimization for likelihood-free inference of simulator-based statistical models. *Journal of Machine Learning Research*, 2016.
- M.U. Gutmann, R. Dutta, S. Kaski, and J. Corander. Likelihood-free inference via classification. *Statistics and Computing*, in press, March 2017. ISSN 1573-1375. doi: 10.1007/s11222-017-9738-6. URL <https://doi.org/10.1007/s11222-017-9738-6>.
- Sepp Hochreiter and Jürgen Schmidhuber. Long short-term memory. *Neural computation*, 9(8):1735–1780, 1997.
- Antti Kangasrääsiö, Jarno Lintusaari, Kusti Skytén, Marko Järvenpää, Henri Vuollekoski, Michael Gutmann, Aki Vehtari, Jukka Corander, Samuel Kaski, et al. ELFI: Engine for likelihood-free inference. In *NIPS 2016 Workshop on Advances in Approximate Bayesian Inference*, 2016. <https://github.com/elfi-dev/elfi>.
- Athanasios Kousathanas, Christoph Leuenberger, Jonas Helfer, Mathieu Quinodoz, Matthieu Foll, and Daniel Wegmann. Likelihood-free inference in high-dimensional models. *Genetics*, 203(2):893–904, 2016.
- Jarno Lintusaari, Michael U Gutmann, Ritabrata Dutta, Samuel Kaski, and Jukka Corander. Fundamentals and recent developments in approximate bayesian computation. *Systematic biology*, 66(1):e66–e82, 2017.
- Paul Marjoram, John Molitor, Vincent Plagnol, and Simon Tavaré. Markov chain monte carlo without likelihoods. *Proceedings of the National Academy of Sciences*, 100(26):15324–15328, 2003.
- Alexander Moreno, Tameem Adel, Edward Meeds, James M Rehg, and Max Welling. Automatic variational abc. *arXiv preprint arXiv:1606.08549*, 2016.
- Krikamol Muandet, Kenji Fukumizu, Bharath Sriperumbudur, Bernhard Schölkopf, et al. Kernel mean embedding of distributions: A review and beyond. *Foundations and Trends® in Machine Learning*, 10(1-2):1–141, 2017.
- Elina Numminen, Lu Cheng, Mats Gyllenberg, and Jukka Corander. Estimating the transmission dynamics of streptococcus pneumoniae from strain prevalence data. *Biometrics*, 69(3):748–757, 2013.
- Jonathan K Pritchard, Mark T Seielstad, Anna Perez-Lezaun, and Marcus W Feldman. Population growth of human y chromosomes: a study of y chromosome microsatellites. *Molecular biology and evolution*, 16(12):1791–1798, 1999.
- William E Ricker. Stock and recruitment. *Journal of the Fisheries Board of Canada*, 11(5):559–623, 1954.
- Scott A Sisson, Yanan Fan, and Mark M Tanaka. Sequential monte carlo without likelihoods. *Proceedings of the National Academy of Sciences*, 104(6):1760–1765, 2007.

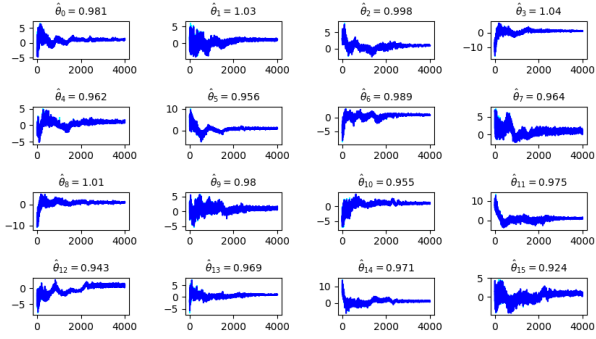


Figure 10: Inferred parameters for one run of ABC-GAN for the multi-variate normal model (Section A). We see that the inferred parameters are close to the true mean  $\mathbf{1}$ .

Bharath K Sriperumbudur, Kenji Fukumizu, Arthur Gretton, Bernhard Schölkopf, Gert RG Lanckriet, et al. On the empirical estimation of integral probability metrics. *Electronic Journal of Statistics*, 6: 1550–1599, 2012.

Didrik F Vestrheim, E Arne Høiby, Ingeborg S Aaberge, and Dominique A Caugant. Phenotypic and genotypic characterization of streptococcus pneumoniae strains colonizing children attending day-care centers in norway. *Journal of clinical microbiology*, 46(8):2508–2518, 2008.

Didrik F Vestrheim, E Arne Høiby, Ingeborg S Aaberge, and Dominique A Caugant. Impact of a pneumococcal conjugate vaccination program on carriage among children in norway. *Clinical and Vaccine Immunology*, 17(3):325–334, 2010.

Simon N Wood. Statistical inference for noisy nonlinear ecological dynamic systems. *Nature*, 466(7310): 1102, 2010.

## A Inference in multi-variate normal

We consider multivariate normal model  $\mathbf{X} \in \mathbb{R}^{16}$  with true mean  $\mathbf{1}$  and prior on mean  $x_i \sim \text{Uniform}(0, 10)$ . We use two layer feed-forward neural networks as our generator and approximator units. A learning rate of  $10^{-3}$  and a hidden layer of size 16 is used in the approximator and generator units. MMD Loss is used as a surrogate for the discriminator as well as for comparing the output of the approximator unit with the simulator.

Figures 10 and 11 show the inferred parameters and the L1-loss between the inferred mean and the true mean as the algorithm progresses. We note that the

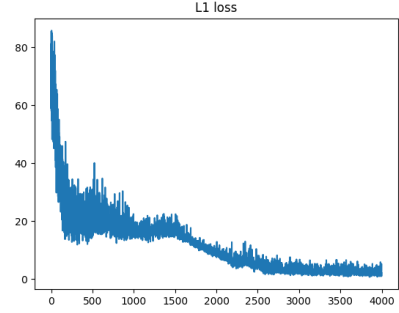


Figure 11: The L1-loss between the inferred and the true mean in the multi-variate normal example (Section A) as the algorithm progresses.

inferred parameters are close to the true mean  $\mathbf{1}$ . The total time taken is 46.38 seconds.

## B ABC-GAN specification for Ricker’s model

This section presents the complete model specification of our GAN architecture for the Ricker’s model. We describe each of the individual sub-networks below.

For sake of completeness, we recall the prior distribution on the parameters  $\theta = (\log r, \sigma, \phi)$  given by:

$$\begin{aligned} \log r &\sim \text{Uniform}(0, 5), \\ \sigma &\sim \text{Uniform}(0, 1), \\ \phi &\sim \text{Uniform}(0, 15). \end{aligned}$$

In the remainder of this section, the notation  $(d = 10)$  indicates the layer has 10-dimensional output.

**Generator** The generator  $G_u(\cdot)$  takes as input the samples from the prior distribution on  $\theta = (\log r, \sigma, \phi)$ . The generator has the following equations:

$$\begin{aligned} x_{G,1} &= \text{ReLU}(w_{g,1}^\top \theta + b_{g,1}) & (d = 20) \\ x_{G,2} &= w_{u,2}^\top x_{g,2} + b_{g,2} & (d = 3) \\ x_{G,3} &= 5 \times \text{Sigmoid}(x_{G,2}[:, 1]) & (d = 1) \quad (\log r) \\ x_{G,4} &= \text{Sigmoid}(x_{G,2}[:, 2]) & (d = 1) \quad (\hat{\sigma}) \\ x_{G,5} &= 15 \times \text{Sigmoid}(x_{G,2}[:, 3]) & (d = 1) \quad (\hat{\phi}) \\ x_G &= [x_{G,3}, x_{G,4}, x_{G,5}] & (d = 3) \quad (\hat{\theta}_{post}) \end{aligned}$$

The complete set of weights are given by  $W_G = \{w_{g,i}, b_{g,i} \forall i \in 1, 2\}$  which are initialized using samples from the normal distribution  $\mathcal{N}(0, 1)$ .

**Approximator** The approximator unit consists of a feed-forward layer which takes as input the posterior parameters  $x_G$  from the generator and outputs

approximate statistics given as:

$$x_A = w_{a,1}^\top x_G + b_{a,1} \quad (d = 3)$$

where the weights  $W_A = \{w_{a,1}, b_{a,1}\}$  are initialized from the normal distribution  $\mathcal{N}(0, 1)$ .

**Summarizer** The summarizer unit consists of LSTM cell followed by a dense layer which projects the sequence to the summary representation. We recall that the standard LSTM unit is defined as:

$$\begin{aligned} f_t &= \sigma(W_f \cdot [h_{t-1}, x_t] + b_f) & (\text{forget gate}) \\ i_t &= \sigma(W_i \cdot [h_{t-1}, x_t] + b_i) & (\text{input gate}) \\ \tilde{C}_t &= \tanh(W_c \cdot [h_{t-1}, x_t] + b_c) \\ C_t &= f_t * C_{t-1} + i_t * \tilde{C}_t & (\text{cell state}) \\ o_t &= \sigma(W_o \cdot [h_{t-1}, x_t] + b_o) & (\text{output}) \\ h_t &= o_t * \tanh(C_t) \end{aligned}$$

where  $W_{LSTM} = \{W_f, W_i, W_c, W_o, b_f, b_i, b_c, b_o\}$  are the weights for a single unit. We use the notation  $LSTM_k$  to denote  $k$  LSTM units connected serially.

Given input sequence  $seq$  obtained from the simulator or from observed data, the summarizer output is given by:

$$\begin{aligned} x_{S,1} &= LSTM_k(seq) & (d = k = 10) \\ x_S &= w_{s,1}^\top x_{S,1} + b_{s,1} & (d = 10) \end{aligned}$$

where the weights are given by  $W_S = \{w_{s,1}, b_{s,1}\} \cup w_{LSTM}$ . The weights are initialized to normal distribution and the initial cell state is set to zero tuple of appropriate size.

**Optimization** The connections are described as follows:

$$\begin{aligned} x_G &= \mathcal{G}(\theta; W_G) \\ x_A &= \mathcal{A}(x_G; W_A) \\ \text{seq}_S &= \text{simulator}(x_G, \epsilon) \\ x_S &= \mathcal{S}(\text{seq}_S; W_S) \\ x_O &= \mathcal{S}(\text{seq}_O; W_S) \end{aligned}$$

where  $\text{seq}_O$  denotes the observed data,  $x_O$  is its summary representation obtained using the summarizer, and  $\epsilon$  denotes normal noise for input to the simulator alongwith the posterior parameter  $X_G$ .

We use maximum mean discrepancy (MMD) loss [Dziugaite et al., 2015] to train the network. Given reproducing kernel Hilbert space (RKHS)  $\mathcal{H}$  with associated kernel  $k(\cdot, \cdot)$  and data  $X, X', X_1, \dots, X_N$  and  $Y, Y', Y_1, \dots, Y_M$  from distributions  $p$  and  $q$  respectively, the maximum mean discrepancy loss is given by:

$$MMD^2[\mathcal{H}, p, q] = E[k(X, X') - 2k(X, Y) + k(Y, Y')].$$

We use the Gaussian kernel and define the following loss functions:

$$\begin{aligned} \mathcal{L}_G &= MMD(x_A, x_O) \\ \mathcal{L}_R &= MMD(x_A, x_S) \end{aligned}$$

Let  $W_R = (W_S, W_A)$  denote the combined weights for the summarizer and the approximator units. The update equations for the network are then given by the following alternating optimizations:

$$\begin{aligned} W_R^{(i+1)} &\leftarrow W_R^{(i)} + \alpha \cdot \text{RMSProp}(\nabla_{W_A, W_S} \mathcal{L}_R) \\ W_G^{(i+1)} &\leftarrow W_G^{(i)} + \alpha \cdot \text{RMSProp}(\nabla_{W_G} \mathcal{L}_R) \end{aligned}$$

where  $\alpha$  is the learning rate for the RMSProp algorithm.

## C Hand-engineered features for the DCC model

Numminen et al. [2013] defined four summary statistics per day care center in order to characterize the simulated and observed data and perform ABC-based inference of the parameters  $\Theta = (\Lambda, \beta, \theta)$ :

- The strain diversity in the day care centers,
- The number of different strains circulating,
- The fraction of the infected children,
- The fraction of children infected with multiple strains.

Gutmann et al. [2017] classified the simulated data as being fake (not having the same distribution as the observed data) or based on the following features:

1.  $L_2$ -norm of the singular values and the rank of the original matrix (2 features),
2. The authors computed the fraction of ones in the set of rows and columns of the matrix. Then, the average and the variability of this fraction was taken across the whole set of rows and columns. Since the average is the same for the set of rows and columns, this yields 3 features.
3. The same features as (2) above for a randomly chosen sub-matrix having 10% of the elements of the original matrix (2 features).

By choosing 1000 random subsets, the authors converted the set of 29 matrices to a set of 1000 seven-dimensional features. This feature set was used to perform classification using LDA. They also did the classification without the randomly chosen subsets mapping

each simulated dataset to a five-dimensional feature vector.

## D ABC-GAN specification for the DCC model

This section presents the complete description for our architecture doing likelihood free inference in the Day-care center example. We describe each of the sub-networks below.

**Generator** The generator  $\mathcal{G}(\cdot)$  takes as input the samples from the prior distribution on  $\Theta = (\Lambda, \beta, \theta)$ . It is specified as follows:

$$\begin{aligned} x_{G,1} &= w_{g,1}^\top \Theta + b_{g,1} & (d=3) \\ \hat{\Lambda} &= 12 \cdot \sigma(x_{G,1}[:, 0]) & (d=1) \\ \hat{\beta} &= 2 \cdot \sigma(x_{G,1}[:, 1]) & (d=1) \\ \hat{\theta} &= \sigma(x_{G,1}[:, 2]) & (d=1) \\ x_G &= [\hat{\Lambda} \ \hat{\beta} \ \hat{\theta}] \end{aligned}$$

The set of variables are given by  $W_G = [w_{g,1}, b_{g,1}]$  which are initialized using normal distribution.

**Approximator** The approximator unit has a feed-forward network given by:

$$x_A = w_{a,1}^\top x_G + b_{a,1}$$

where  $W_A = [w_{a,1}, b_{a,1}]$  are the weights which are initialized using the normal distribution.

## E Supplemental Figures

- Figure 12 shows the inferred parameter values in Section 4.1.3 of the main manuscript. The true parameter is  $\mathbf{0}$  with prior  $\theta_i \sim \text{Uniform}(-100, 100)$  and two layer feed-forward networks used for the generator and approximator in the ABC-GAN structure.

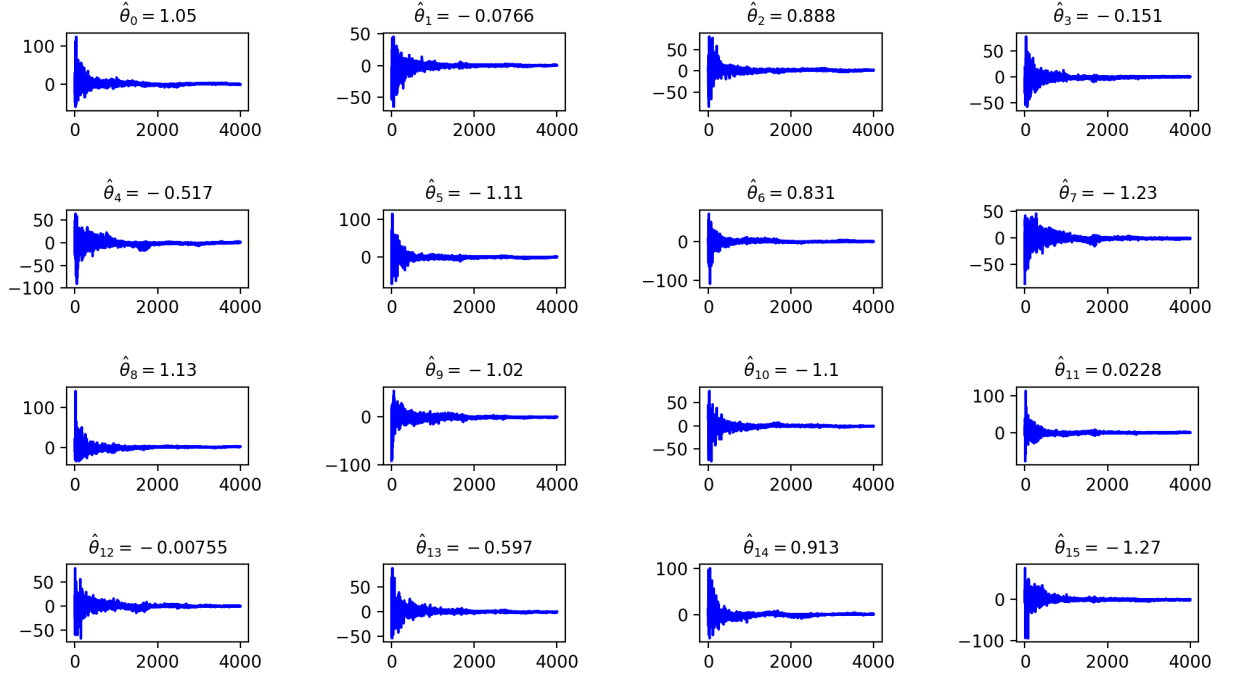


Figure 12: Inferred parameter values (true parameter is  $\mathbf{0}$ ) with prior  $\theta_i \sim \text{Uniform}(-100, 100)$  and two layer feed-forward networks used for the generator and approximator in the ABC-GAN structure.